PRAMANA
— journal of
physics

Vol. 56, No. 5
May 2001
pp. 667–684

Experimental evidence of photoinduced valence change of Fe^{3+} in $BaTiO_3$ and mechanism for growth of new grating in depleted pump condition: An EPR investigation

M D SASTRY*, M MOGHBEL, PUTCHA VENKATESWARLU† and A DARWISH
Department of Physics, Alabama A&M University, Normal, Alabama 35762, USA
*Radiochemistry Division, Bhabha Atomic Research Centre, Mumbai 400 085, India
Email: mdsastry@magnum.barc.ernet.in
†Deceased

MS received 5 August 2000; revised 1 February 2001

Abstract. With a view to understanding the role of photo-induced valence changes of impurities in $BaTiO_3$ in the phenomena of photorefraction, EPR experiments were conducted under *in situ* He–Ne laser illumination. These experiments gave evidence for photoinduced valence change of Fe in $BaTiO_3$ at room temperature. The EPR signal due to trivalent iron was found to reduce in intensity with laser illumination The kinetics of the valence change has been investigated. Under large fringe width condition, the time constant of the decay is identified as the dielectric relaxation time τ_d. The changes in line shape on laser illumination to Dysonian form, appeared most predominantly in mechanically poled crystal compared to electrically poled single domain crystals. This demonstrated the possible role of domain walls and the defects there, as source or sinks of charge carriers on photo excitation. It is observed, that there is transient growth of Fe^{3+}, when the laser illumination was put on, before its decay. This was attributed to charge transfer between electrons in oxygen vacancies and Fe^{4+}. This predicted the growth of a transient grating under depleted pump condition in a two beam coupling experiment. This was experimentally proved by following the diffracted signal of the reading beam under the depleted pump condition.

Keywords. Photorefraction; electron paramagnetic resonance of Fe^{3+}; $BaTiO_3$; photo-electron paramagnetic resonance.

PACS Nos 76.30.Fc; 78.20.Jq; 42.70 Ln; 42.70 Nq

1. Introduction

The photorefractive effect (light induced change in refractive index) in ferroelectric crystals such as lithium niobate ($LiNbO_3$) and barium titanate ($BaTiO_3$) has been identified [1] as due to charge transport during nonuniform illumination, from the more illuminated to the less illuminated regions. Such a charge transport would result in a spatially modulated charge distribution when an interference pattern is produced in the crystal. The resulting space charge field then modulates the refractive index of the materials and in conjunction with the Pockel effect, leads to the formation of phase grating [1]. Under the assumption

of a single type charge carrier, the photorefractive effect and beam couplings have been explained using band conduction [2–4] and hopping [5] models. Even though it was noted that both electron and hole conduction simultaneously takes place, the sign of charge carriers is taken as that of the majority carriers, signifying that only the net average charge mobility is taken into account. The sign of the charge carriers can be determined from the sign of the beam coupling coefficient 'Γ', [1] particularly in electrically poled crystals of $BaTiO_3$. However in $BaTiO_3$ crystal, the sign of the charge carriers and that of 'Γ' were observed to be sample dependent [6]. Strohkendl *et al* [7] have shown that in nearly compensated $BaTiO_3$, the sign of the space charge field, and thereby the sign of beam coupling coefficient, change beyond a certain value of the grating wave vector **k**. This was attributed to the competition between electron and hole mobilities. The charge transport, in photo excited $BaTiO_3$ has been attributed to an extrinsic iron impurity and in chemical terms, the e^- and h^+ mobilities, respectively were identified to be associated with the oxidation of Fe^{2+} or reduction of Fe^{3+} on photo excitation of Fe : $BaTiO_3$ [7]. Schunemann *et al* [8] have shown that the valence of the iron impurity changes as a function of oxygen partial pressure PO_2 in the range of $1–10^{-4}$ atm. Garrett *et al* [9] have shown that the presence of another iron group element cobalt, increases the electro-optic coupling of $BaTiO_3$. In view of these and similar findings it became increasingly obvious that extrinsic defects and their chemical nature in general contribute to a number of features in the photorefractive effect and associated phenomena in crystalline $BaTiO_3$. The identification of the role of specific impurities is therefore important both for understanding the mechanism of photorefraction as well as for optimizing the growth conditions of photorefractive crystals for specific applications. Among the extrinsic defects, ions of iron group are expected to be common ones even in nominally pure crystal.

A number of transition metal ions are paramagnetic and the expected concentrations in $BaTiO_3$ are typically few tens of parts per million. Electron paramagnetic resonance (EPR) spectroscopy is an established technique [1] to characterize these impurities for their valence state, site symmetries and associated lattice (point) defects, and also for photo induced valence changes. In fact EPR is ideally suited for the detection of Cr^{3+}, Fe^{3+}, Mn^{2+}, Mn^{4+} and Cu^{2+} impurity ions. This technique however suffers from the disadvantage that those valence states of ions having large orbital contributions to their ground state magnetism can be detected only at low temperatures (typically 20 K or less) due to their short spin-lattice relaxation time. (Typical examples are V^{3+}, Mn^{3+}, Fe^{2+}, Ni^{2+}, high spin Co^{2+} and Ni^{3+}.)

Photoinduced valence changes of transition metal impurities in $BaTiO_3$ were investigated by Possenriede *et al* [11–13] and Schwartz and coworkers [14–17] at low temperatures in the rhombohedral phase. The investigations of Possenriede *et al* [11–13] have shown that the photoinduced changes depend upon the sample history with regard to laser illumination. These authors concluded that hole ionization of Fe^{4+} is the dominant photoinduced valence change involving iron impurity. Schwartz and coworkers [14–17] have obtained a clear evidence of charge transfer from the paramagnetic Co^{2+}, Fe^{3+} and O^- by conducting '*in situ*' EPR studies during laser illumination. These measurements were carried out at 45 and 25 K, in the rhombohedral phase of the host lattice, $BaTiO_3$. Even though the ambient temperature in these experiments was far below the room temperature where photorefractivity experiments are usually conducted, the experiment below 45 K helped in identifying the role of Co^{2+}, Fe^{3+} and O^- (whose EPR can be best observed mostly at low temperature due to relaxation and/or thermal stability reasons), in the photo-

induced charge transfer processes. It may be pointed out that the work of Schwartz *et al* [17] has shown an interesting temperature dependence of photo induced changes in the 45–25 K range. Whereas at 25 K, the photo induced effects enhanced Co^{2+} concentration, the opposite effect was observed at 45 K. In a subsequent investigation Schwartz *et al* [18], using photo-EPR measurements, have provided definite evidence for the optical activity of V^{3+} in CdTe under sub-band-gap illumination. Whereas the photorefractive measurements carried out at room temperature implied that the charge carriers in CdTe were electrons, the photo-EPR measurements at 5 K suggested that the photoionization of hole from V^{3+} was responsible for charge transport. This discrepancy was attributed to the differences in temperature at which photorefractive and EPR measurements were conducted. These results highlight the complexities of photo-induced ionization and hopping transport in photorefractive crystals suggesting that it may be worthwhile to conduct these experiments closer to room temperature, to probe the photo-induced electron transfer relevant to photorefraction at room temperature. Furthermore, in crystals undergoing successive phase transitions, the low temperature phase is not expected to be of single domain [19] and the defects at the domain boundaries are expected to contribute to the complex behavior. With a view to minimizing the role of such unavoidable effects, and also to understand the processes that happen at room temperature, we have conducted *in situ* EPR investigations under He–Ne laser illuminations on mechanically poled and electrically poled $BaTiO_3$ crystal in which Fe^{3+} and Cu^{2+} were found to be paramagnetic impurities. In view of the piezoelectric nature of $BaTiO_3$ the photoinduced valence changes and associated local strains play a crucial role in the efficiency of grating formation [20], and this information can be obtained by photo-EPR studies.

These experiments have given evidence to suggest that Fe^{3+} ions do take part in photo-induced charge transfer at room temperature, and also show a marked variation in its behavior in a narrow temperature range around the ambient. These experiments also gave evidence for the possible role of domain boundaries, and of nonuniform illumination on charge transfer, especially in mechanically poled crystals. Furthermore, these investigations lead to the understanding of a possible physical mechanism for the transient growth of a grating under the depleted pump condition in a normal two beam coupling experiment.

2. Experimental

Experiments were conducted on three commercially available $BaTiO_3$ crystals (supplied by Lockheeds-Nashua, NH, USA), one mechanically poled and two electrically poled crystals. These crystals were designated M1, E1 and E2. (These crystals were obtained at different times and were from different lots. The crystal M1 was found to contain Cu^{2+} impurity in addition to Fe at much higher concentration.) Among the electrically poled crystals, the crystal E2 has shown poorer photo-refractive behaviors viz lower beam coupling and phase conjugation efficiency. The crystals were grown in air (PO_2=0.21).

EPR studies were conducted on a Bruker ESP-300E X-band spectrometer operating around 9.3–9.5 GHz, equipped with an optical transmission cavity. Some of the preliminary experiments were conducted on a Varian Century X-band spectrometer, at the Department of Chemistry, University of Alabama at Tuscaloosa, using a homemade optical transmission cavity. The optical illumination was done using a 35 mW He–Ne laser.

Standard two beam coupling experiment was conducted using a 50 mW He–Ne laser, to investigate the growth of transient grating under depleted pump conditions. The experimental setup is described in greater detail elsewhere [21]. The writing and reading beams are designated as A_1 and A_2 respectively. The transmitted/diffracted beams were detected using photodiodes (PIN 10DP supplied by United Detector Technology). The growth and decay of these signals were monitored by feeding the output of the photodiodes to HP 7090A digital plotter.

3. EPR characterization of impurity centers in barium titanate

The investigated crystals, were nominally pure with no intentionally doped impurities. The EPR experiments have however shown that all the crystal contained iron impurity, and the mechanically poled crystal contained an additional copper (2+) impurity. The type of impurity present has no relation to the mode of poling the crystals.

Unlike the EPR of Fe^{3+} in $BaTiO_3$, where exhaustive work has been reported [19, 22–25] EPR studies of Cu^{2+} have not been reported except for a brief mention of the EPR detection of Cu^{2+} in one of the crystals (BW1) used by Klein and Schwartz [14]. In this report we describe the results of our EPR investigations of Fe^{3+} in two crystals and Cu^{2+} in a mechanically poled $BaTiO_3$ crystal. It was more difficult to tune the spectrometer and obtain a good AFC lock for the mechanically poled crystal compared to the electrically poled one and further the line shapes were more asymmetric for the mechanically poled sample. This appears to be due to larger number of defects in M1 (at domain boundaries) in view of incomplete poling. These defects take part in photo/thermal induced charge transfer. This has been solved by taking smaller samples.

3.1 *Fe^{3+} center in $BaTiO_3$*

Figures 1a, b and 2a, b show the EPR spectrum obtained for crystals M1 and E1 for the magnetic field parallel to c-axis and a or b axis respectively. The lines marked $a1$ to $a5$ are the five fine structure transitions of Fe^{3+} which agree with those reported by Klein and Schwartz [14] for Fe^{3+} at the Ti^{4+} site with no nearby charge compensating defects. In addition to Fe^{3+}, Cu^{2+} impurity was detected in M1 and this spectrum will be discussed in the next subsection.

The electrically poled crystal E1 was of single domain. The angular variation of these Fe^{3+} spectral lines in (a, c) plane agrees satisfactorily with that reported by earlier workers [14, 19–22] and is shown in figure 3. The spectrum can be fitted to the axial spin Hamiltonian, with the usual notation [10]:

$$H = g\beta H \cdot s + D[3S_z^2 - S(S+1)] + a[S_x^4 + S_y^4 + S_z^4 - (1/5)S(S+1)(3S^2 + 3S - 1)]. \quad (1)$$

The spin Hamiltonian constants were obtained by using the field values for $H_{\parallel}c$ and $H_{\perp}c$. The values obtained are:

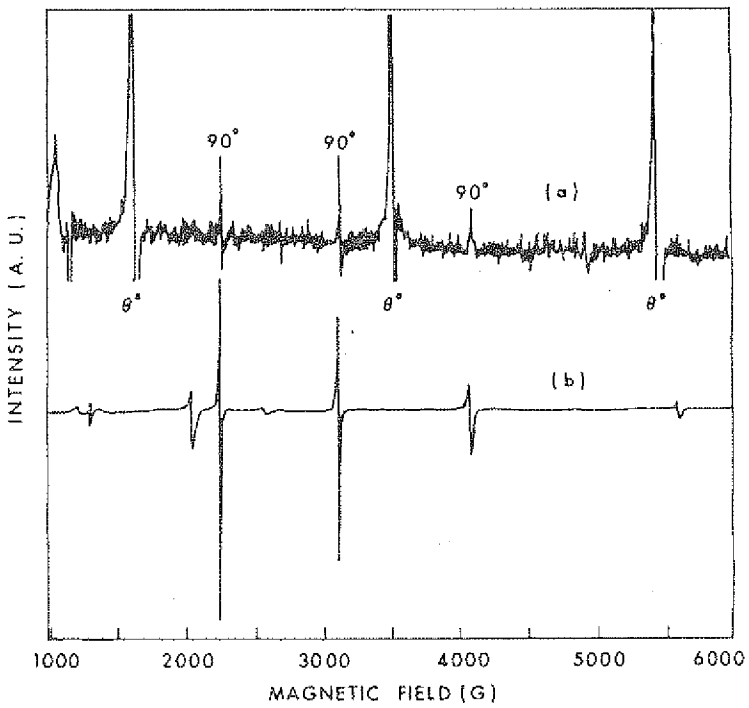

Figure 1. EPR spectrum obtained for $BaTiO_3$ crystal (M1) at room temperature: (a) magnetic field parallel to c-axis, (b) magnetic field parallel to a/b-axis. The presence of 90° domains is seen by the existence of 90° spectra in (a).

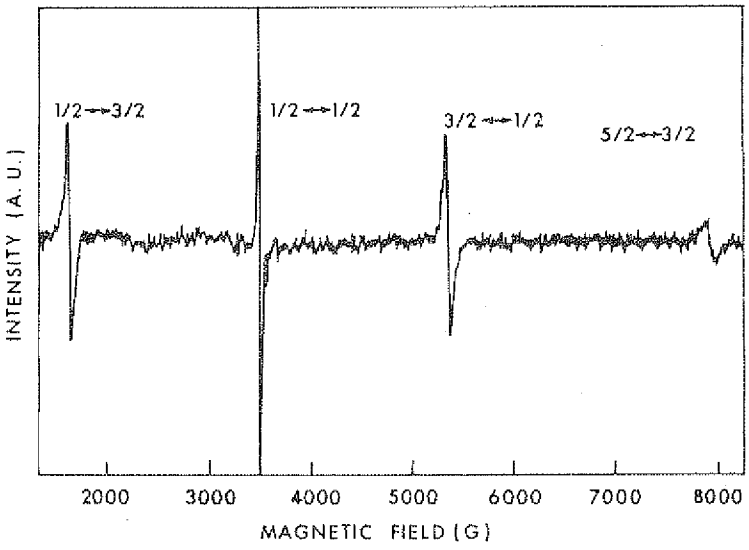

Figure 2a. EPR spectrum obtained for electrically poled $BaTiO_3$ crystals, magnetic field parallel to c-axis.

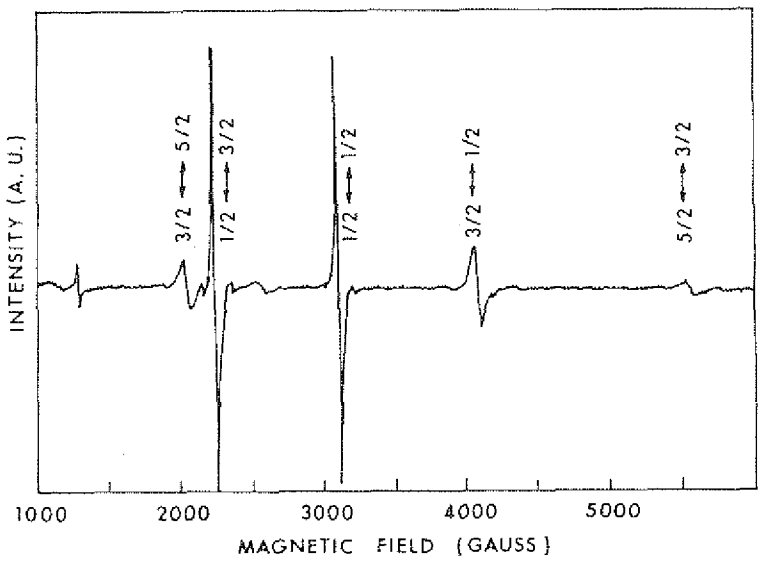

Figure 2b. EPR spectrum obtained for electrically poled $BaTiO_3$ crystals, magnetic field parallel to a-axis.

$$g_{\|} = g_{\perp} = 2.003 \pm 0.001,$$
$$D = 1055 \pm 5G,$$
$$a = 96 \pm 2G.$$

These values compared very satisfactorily with those reported in the literature [19,22]. The central $\pm 1/2 \rightarrow \pm 1/2$ transition which is expected to be nearly angular independent for Fe^{3+} ions at axial sites shows a strong angular dependence, particularly for the direct ion of H close to the $\langle 110 \rangle$ axis. This is due to the relatively large value of D and obeyed the expression

$$H_{1/2 \rightarrow -1/2} = H_0 + 2D^2/(g\beta)^2 H_0[8 \sin^2 \Theta \cos^2 \Theta - \sin^4 \Theta] \qquad (2)$$

where Θ is the angle, the direction of the magnetic field makes with the c-axis. However, one anomalous feature of the $+1/2 \longleftrightarrow -1/2$ transition is, its apparently large intensity compared to the expected intensity ratio of $5:8:9:8:5$ with other fine structure transitions which can partly be accounted for by the larger line widths of other transitions. This suggests that there exists inherent crystal field inhomogeneties even in high optical quality electrically poled crystals.

When Fe^{3+} enters the lattice substitutionally at the Ti^{4+} site, some of the Fe^{3+} ions may be associated with oxygen vacancies for charge compensation. Such a center is designated as $[Fe^{3+} - V_0]$ center. Such centers were most exhaustively studied in Fe^{3+} doped $StTiO_3$ [26,27]. When Fe^{3+} is associated with an oxygen vacancy in the first coordination sphere, the ion will be subjected to a very strong axial distortion and the three Kramers' doublets arising from the ground ^6S state will have a separation significantly larger than the microwave energy ($0.3\ cm^{-1}$) used. EPR in such cases will be observable only if $|\pm 1/2\rangle$ state lies lowest. In this state g-values will have the form $g_{\|} = g_j$ and $g_{\perp} = 3g_j$.

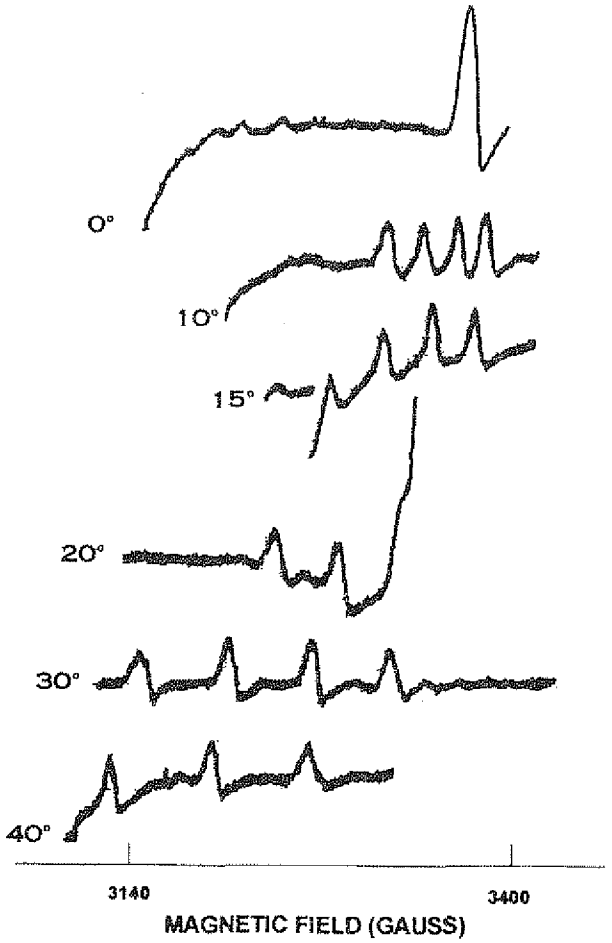

Figure 3. Angular variation of the EPR spectrum of Cu^{2+} impurity in $BaTiO_3$ M1 in (a, c) plane.

The line marked 'V' in this spectrum has g value of 5.98. Its angular variation could not be followed for all angles. This line together with significantly large intensity of $1/2 \rightarrow -1/2$ for $H_{\|}c(g = 2)$ suggest a possible species with effective spin $S' = 1/2$ with g values $g_{\|} = 2.00$ and $g_{\perp} = 5.98$. This can possibly be assigned to the $(Fe^{3+} - V_0)$ center in $BaTiO_3$. In addition to this an extra resonance around 650 G also was observed. It was most likely a forbidden transition of the type $\Delta M_s = \pm 2$ in Fe^{3+} at Ti^{4+} site without a nearly oxygen vacancy.

3.2 *EPR of Cu^{2+} in $BaTiO_3$*

In addition to the intense spectrum due to Fe^{3+} a weaker but sharper spectrum due to Cu^{2+} ion was detected. It has the characteristic quartet hyperfine structure with partly resolved

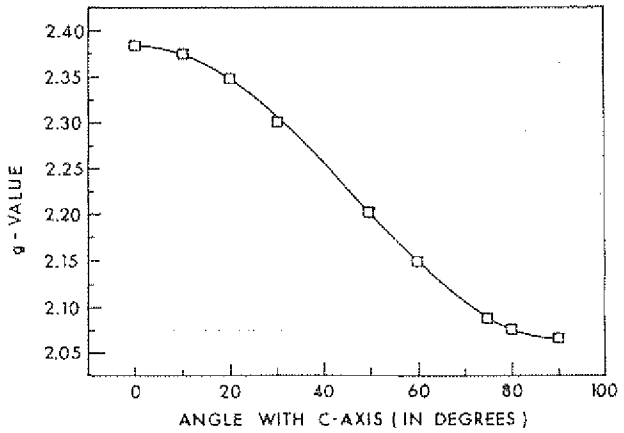

Figure 4. Angular variation of the g-tensor for Cu^{2+} in $BaTiO_3$ (M1). The solid line is theoretical line and the points are experimental points.

isotope structure expected due to ^{63}Cu and ^{65}Cu (both have $I = 3/2$). The g-value and hyperfine coupling constant were found to be isotropic in $[a, b]$ plane, but highly anisotropic in $[a/b, c]$ plane. Therefore the site symmetry of the Cu^{2+} ion is found to be tetragonal with principal axis along the c-axis. The spectrum of Cu^{2+} can be seen in figure 1a for M1 sample with the magnetic field parallel to c-axis. Free Cu^{2+} ion has the outer electronic configuration of $3d^9$ and when placed in an octahedral crystal field has the form $t_{2g}^6 e_g^3$. When the octahedral symmetry is lowered due to an axial distortion, the lowest electronics state was an orbital singlet and it facilitated the observation of EPR over a wide temperature range. The electronic wave function would either be $(x^2 - y^2)$ or $(3z^2 - r^2)$ depending upon whether the octahedron is elongated or compressed, respectively. These two cases can be distinguished by EPR, from the relative values of the principal components of the g-tensor. In the case of the $|x^2 - y^2\rangle$ state, i.e., when the octahedron was elongated along one direction the principal g-values follow the pattern $g_\parallel > 2 > g_\perp > 2$. On the other hand, in the case of $|3z^2 - r^2 >$ state, i.e., when the octahedron is compressed along one direction the principal components of the g-values follow the pattern $g_\perp > 2 > g_\parallel$ [10].

The spectrum of Cu^{2+} is shown in figure 4 for different angles with the magnetic field with c-axis in $[a, c]$ plane. The spin Hamiltonian parameters of the Cu^{2+} sites are:

$$g_\parallel = 2.383 \pm 0.001,$$
$$g_\perp = 2.066 \pm 0.0001,$$
$$A_\parallel = 97 \pm 1 \text{ Gauss},$$
$$A_\perp \sim 5 \text{ Gauss}.$$

The line positions and hyperfine coupling constants at any angle can be satisfactorily predicted using the principal values of the g and A tensors. It is important to note that the principal axis system of the g and D tensors of Fe^{3+} at the octahedral site coincide with those of the g and A tensors of Cu^{2+}. The correctness of the values obtained for the principal axis systems were checked by comparing the g and hyperfine coupling constant values for any arbitrary angle Θ with the expected values.

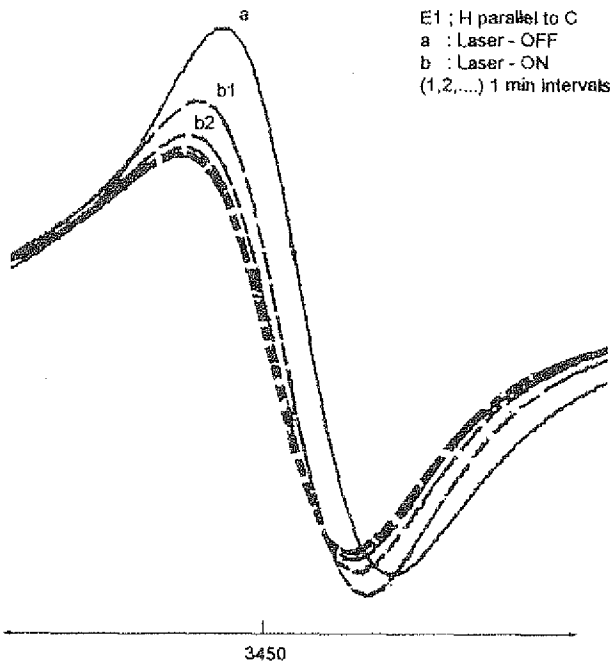

Figure 5. Effect of He–Ne laser illumination on the $1/2 \longleftrightarrow -1/2$ line of Fe^{3+} in E1.

The hyperfine coupling constants $K(\Theta)$ and $g(\Theta)$ in their respective principal axis systems are given by the expressions [10]

$$K^2 g^2 = A_{\parallel}^2 g_{\parallel}^2 \cos^2 \Theta + A_{\perp}^2 g_{\perp}^2 \sin^2 \Theta \tag{3}$$

and

$$g^2 = g_{\parallel}^2 \cos^2 \Theta + g_{\perp}^2 \sin^2 \Theta. \tag{4}$$

The fitting between the observed and expected values of $K(\Theta)$ and also of $g(\Theta)$ were quite satisfactory. The angular variation of $g(\Theta)$ is shown in figure 5, the points shown are experimental points and the curve is the calculated one using the $g_{\parallel}$ and $g_{\perp}$ values given above.

The experimentally obtained values of $g_{\parallel}$ and $g_{\perp}$ as 2.383 and 2.066 respectively, suggest that $[CuO_6]^{10-}$ is elongated along the z-axis (or compressed along the x and y axis). This clearly suggest that substitution of Cu^{2+} at the Ti^{4+} site produced local distortion of the regular $[TiO_6]^{9-}$ octahedron.

4. Effect of *in situ* laser illumination

EPR investigations were carried out during illumination with a He–Ne laser light. This work was performed, to examine *in situ* the photoinduced charge transfer form Fe^{3+} in

the $BaTiO_3$ crystal lattice, as this was generally accepted to be a key step in inducing photorefractive behavior of $BaTiO_3$ crystal. These experiments were carried using an optical transmission cavity (Bruker model, E4104 or) on sample M1 and E1.

The measurements were carried out under the following two experimental conditions:

(i) Sample loaded in an optical transmission cavity was uniformly illuminated by light from a He–Ne laser with Gaussian profile of the laser beam, and also after beam expansion and collimation.

(ii) The sample was half covered by black paper and illuminated by laser light, essentially to stimulate the condition of an interference pattern with a large fringe width (or grating period).

4.1 *Mechanically poled crystal M1*

The crystal was illuminated in the optical transmission cavity. Figure 6a shows the change in the intensity of $1/2 \longleftrightarrow -1/2$ transition for $H \| c$ after the laser was switched on at different time intervals in steps of half a minute and figure 6b shows the relaxation back to its original form after the laser was switched off. It can be seen that the intensity of the line goes down with laser illumination, along with a concomitant change in line shape

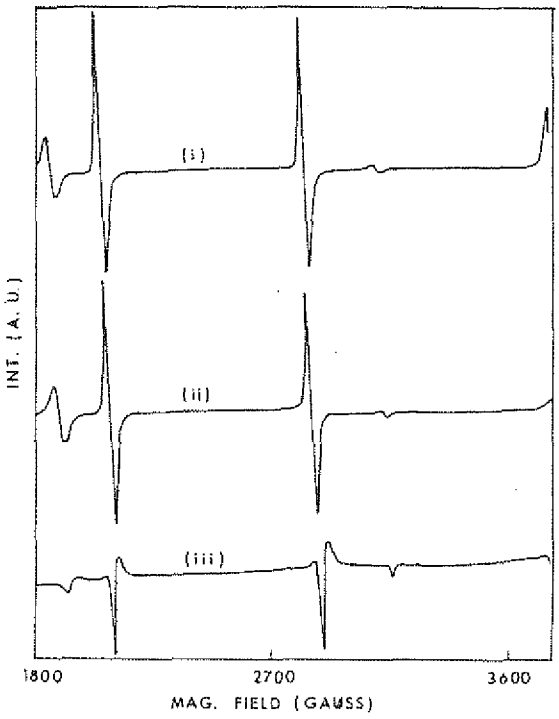

Figure 6. Effect of He–Ne laser illumination on the EPR of Fe^{3+} in M1. (i) No illumination, (ii) uniform illumination, (iii) nonuniform illumination (half bright-half dark).

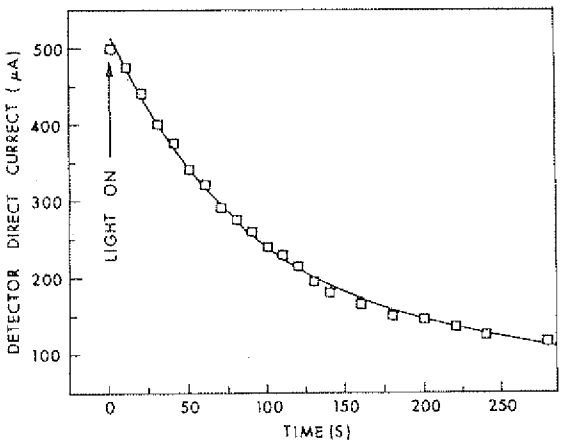

Figure 7. Time dependent changes of the detector current with nonuniform illumination of M1 crystal.

with time. This change was found to be reversible, with the line regaining its original intensity and shape after the laser was switched off (see figure 6b). To examine whether the change in the line shape towards Dysonian form was due to nonuniform illumination arising from the Gaussian profile of the laser beam, the beam was expanded and collimated. Under these conditions of uniform illumination, the changes in the line shape were found to be much less prominent. In view of the observed effect of nonuniform illumination (see figure 6) and with a view to simulating the condition of interference pattern (of course with an extremely large fringe width), half of the crystal was blocked during the laser illumination under expanded beam condition. Figure 7a, b and c show the EPR of M1 crystal with $H_{\perp}c$, with no laser illumination, with uniform illumination and non-uniform illumination (half bright and half dark), respectively. The drastic change in line shape when only half the crystal is illuminated can be seen in figure 7c. Under the condition of half bright and half dark illumination, the detector current showed prominent time dependent increase, and it was found to be reversible, reverting back to its original value after the laser was switched off. The changes were highly reproducible. Figure 8 shows time dependence of detector current during non-uniform (half bright and half dark) illumination.

The time dependent changes in intensity of the Fe^{3+} spectrum during uniform illumination was investigated, by locking the magnetic field on the peak position of one of the fine structure transitions of Fe^{3+}. Figure 9 shows the recovery and decay of Fe^{3+} signal with laser off and laser on condition. An interesting observation in these measurements is a small but definite surge in the intensity of Fe^{3}, soon after the laser was on. The EPR spectrum of Cu^{2+} also shows changes in intensity with laser illumination.

4.2 *Electrically poled crystal E1*

Experiments similar to those described above on M1 were conducted with the crystal E1. An important distinguishing feature of the electrically poled crystal is that the line shape did not change as in the case of M1, when illuminated with Gaussian profile from He–Ne

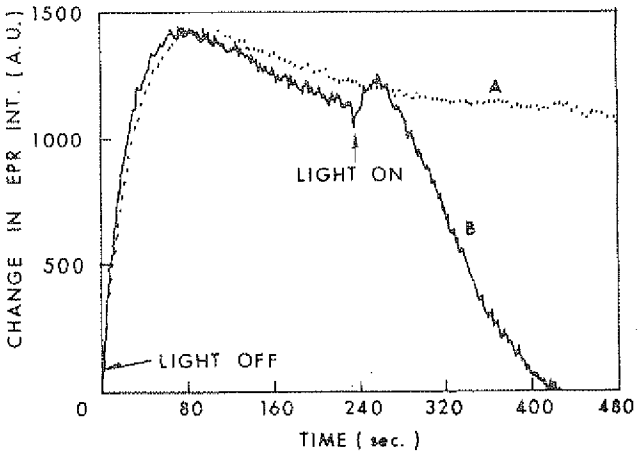

Figure 8. Kinetics of decay and recovery of Fe^{3+} signal in M1 (under uniform laser illumination).

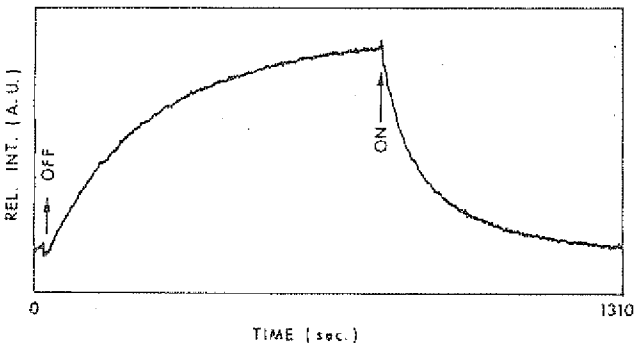

Figure 9. Decay kinetics of and recovery of Fe^{3+} signal in E1 (under uniform illumination).

laser light. The intensity of the Fe^{3+} lines, however, was found to decrease with laser illumination. When the illumination was made highly nonuniform, with bright and dark regions as in the case of M1, the line shape was found to become asymmetric, but the difference was much less drastic compared to that in the case of M1. Figure 10 shows the time dependence of the decay and growth of Fe^{3+} with and without laser illumination respectively. In a significant number of experiments with E1, it was observed that a surge in the Fe^{3+} intensity occurred when the laser was switched on before it started decaying.

4.3 *Analysis of time dependence of growth and decay of* Fe^{3+}

The time dependence of intensity of EPR spectrum with and without laser illumination was fitted using standard expressions characterizing the single and/or double exponential decay

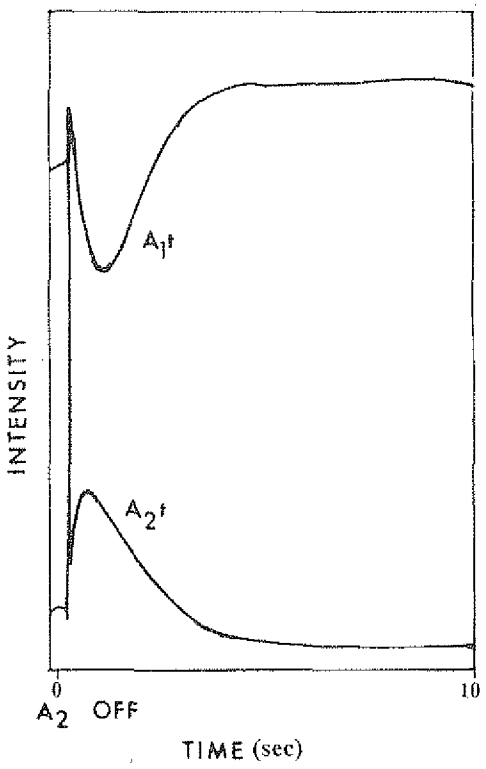

Figure 10. Time dependence of the transimitted beam intensity of writing beam A_1t after the second beam was switched off. The initial decay of A_1t and associated increase of the diffraction signal clearly shows the grating formation after the second beam A_2 was switched off.

and growth respectively. Best fits were observed for single exponential in case of the decay of the signal, and a double exponential in case of the growth of the signal.

$$I_{\text{decay}} = I_0 + A\exp[-(t-t_0)/\tau_1], \tag{5}$$

$$I_{\text{growth}} = B + C\{1-\exp[-(t-t_0)/\tau_2]\} + D\{1-(t-t_0)/\tau_3], \tag{6}$$

where A, B, C and D are constants: and τ_1, τ_2 and τ_3 are time constants characterizing the respective time dependencies. The values of τ_1, τ_2 and τ_3 are the parameters obtained in different conditions are given in table 1.

5. Discussion

From the experimental results described above the most important observations may be summarized as:

(a) Charge transfer on photo excitation does result in the valence change of iron impurity, which gives direct evidence about the photorefractive nature of the Fe center at room temperature, even wih He–Ne laser.

Table 1. Time constants characterizing the time dependent changes in EPR measurements with laser illumination of Fe^{3+}: $BaTiO_3$.

Sample	Experimental condition	Property monitored	Time Constant (sec) decay	growth
Mechanically poled crystal (M1)	Uniform laser illumination	Intensity of Fe^{3+} signal	85.5	97.6, 25 (Double exponential)
-do-	Non-uniform illumination (half bright and half dark)	Detector current	97.6	97.6
Electrically poled crystal (E1)	Uniform illumination	Intensity of Fe^{3+} signal	166	100, 24 (Double exponential)

(b) There is a distinct difference in the behavior of mechanically and electrically poled crystals with regard to change in line shape on laser illumination. In a mechanically poled crystal, the change of line shape to the Dysonian form is very prominent compared to that in a single domain electrically poled crystal.

(c) The decay time constant (τ) data observed under different conditions, suggest that predominantly there are two charge transfer processes in $BaTiO_3$ when illuminated with 633 nm light, with characteristic time constants around 100 ± 10 sec and 26 ± 2 sec. These time scales are significantly greater than those reported in the case of optical experiments.

(d) In the study of kinetics of valence change, a 'surge' (a sharp but small rise) in the concentration of Fe^{3+} was observed before the onset of decay of the Fe^{3+} signal, during laser illumination.

5.1 *Photo-induced valence changes*

It has been conjectured for quite some time that the Fe-center does play an important role as a photorefractive center in $BaTiO_3$:Fe. The direct experimental evidence was obtained in the EPR study of Schwartz *et al* [17] and Possenriede *et al* [12,13], where it was shown that laser illumination at 25 K results in increase in the relative concentration of Fe^{3+}. The observation (a) mentioned above gives direct evidence of a photo-induced valence change of Fe in $BaTiO_3$ right at room temperature but of a reverse type, i.e., reduction in Fe^{3+} concentration with laser illumination. As mentioned earlier, the crystal investigated were grown in air, where the partial presence of oxygen $PO_2 = 0.21$. Wechsler and Klein [28] have shown that at this value of PO_2 the Fermi level in $BaTiO_3$ will be closer to the Fe^{3+}/Fe^{4+} ionization level where Fe^{3+} acts as a donor and Fe^{4+} acts as an acceptor. If the Fermi level (E_F) is lower than the ionization energy of Fe^{3+}, E (Fe^{3+}/Fe^{4+}), the stability of valence state of Fe will be more towards tetravalency. On the other hand, if E_F is higher than the ionization energy of Fe^{3+}/Fe^{4+}, then the stability of the iron valence is more towards trivalency.

At room temperature E_F and E (Fe^{3+}/Fe^{4+}) are close [28], and therefore there is tendency of stabilization of Fe^{4+}, and hence under photo-illumination there will be a greater tendency for the ionization of Fe^{3+}.

5.2 *Sample dependence of EPR*

The second observation, (b), above suggests strong sample dependence of EPR. The Dysonian form of the line shape in the figures, clearly shows that a bulk microwave loss has come into play during nonuniform illumination of M1. This has to be either due to the onset of electrical conductivity or significant change in dielectric properties. The latter is not known to happen and the former is more physically consistent with possible photoconduction in $BaTiO_3$.

The domain boundaries which are expected to be more in numbers in the mechanically poled crystal compared to one electrically poled, and the defect state associated with them play a predominant role as source/sink of charge carriers released on photoexcitation. This results in the local photo currents which in turn become sources of additional microwave dissipation resulting in changes in the detector current. This aspect of the present work is important to realise the limitation of relating the photo-EPR data reported at 25 K [17] to the optics experiments at room temperature. In view of the successive phase transitions that $BaTiO_3$ undergoes before finally entering the rhombohedral phase at 25 K, the crystal would be far from being a monodomain crystal and will have a large number of domain boundaries and associated lattice defects. Therefore, the information obtained in the rhombohedral phase can not be extrapolated to the room temperature tetragonal phase of $BaTiO_3$.

5.3 *Decay and growth behavior*

Table 1 gives the values of τ_1, τ_2 and τ_3 characterizing the decay and growth of Fe^{3+} signal (see eqs (5) and (6)) in M1 and E1 crystals. From table 1 it can be seen that the charge transfer process on illumination with He–Ne laser, resulting in the valence change of Fe^{3+} had a characteristic time of around 100 s in M1, whereas it was nearly double that in case of E1. The shorter time in the case of M1, appears to be due to the presence of multidomains and therefore defects at domain walls, which quickly trapped the electrons or holes.

In general, it appears that relaxation process, as viewed from the change in EPR of Fe^{3+}, has two characteristic time constants. The faster process characterizes the charge relaxation back to pre-exposure. It is known [29] that under the condition of infinitely large fringe width, the grating erasure rate becomes equal to the dielectric relaxation rate. Under the present experimental conditions $\tau = 25$ s and may be identified with dielectric relaxation rate τ_d which for $BaTiO_3$ sets the slowest limit for the grating erasure time. The dielectric relaxation time τ_d is given by [26]

$$\tau_d = \epsilon\epsilon_0/(n_d + n_L)\mu e = \epsilon\epsilon_0/\sigma,$$

where ϵ and ϵ_0 are the dielectric constant of $BaTiO_3$ and permitivity of free space, respectively, $(n_d + n_L)$ are the number of free charge carriers during photoexcitation, μ is the

charge mobility, and e is the electron charge. Ducharme and Feinberg [30] have estimated the value τ_d, by extrapolating the dark decay rate vs spatial frequency square, to $k \to 0$ limit. This was found to be equal to 0.5 s which in turn gave a value of conductivity $\sigma = 10^{-11}$ $(\Omega\ \mathrm{cm})^{-1}$. As the grating vector, in the measurements of Ducharme and Feinberg [30] was parallel to c-axis, they used the value of $\epsilon = \epsilon_c = 150$, for determining the value of σ in $BaTiO_3$.

In the present experiments the crystal was illuminated either uniformly or with no specific direction of $\mathbf{k}$ when it was nonuniformly illuminated. Therefore, it may be more realistic to take an average value $[1/3](\epsilon_a + \epsilon_b + \epsilon_c) = 2440$ for the dielectric constant. For τ_d value of 25 s, and $\epsilon = 2440$, the conductivity σ was estimated to be 0.8×10^{-11} $(\Omega\ \mathrm{cm})^{-1}$. This is in general of the same order of magnitude of σ reported in $BaTiO_3$ [30]. The slower parts of the relaxation with a time constant of ~ 100 s is most likely the relaxation in the immediate environment at Fe-site, undergoing valence change, due to Sangster effect [20].

5.4 *Surge in Fe^{3+} under depleted pump condition and mechanism of growth of transient grating*

Another interesting observation in these experiments is the sudden surge in the intensity of Fe^{3+}, in high temperature range, immediately after the laser was switched on, before subsequent decay of Fe^{3+}. In what follows possible reasons are suggested for this observation, which involve an interplay between photoinduced electron transfer between point defects and the relative stabilities of valence states of Fe dictated by the mode of charge compensation.

The kinds of impurities and other point defects, potentially acting as photorefractive centers, in $BaTiO_3$ and their energy levels were discussed by Klein [31]. The iron impurity with its ability to exist in different valence states, 2+, 3+ and 4+ at Ti^{4+} site, behaves both as donor and acceptor. The existence of Fe in valence states less than 4+ would produce oxygen vacancies V_O for charge compensation, their numbers increasing with the concentration of Fe^{2+} and to a lesser extent with that of Fe^{3+}. These vacancies serve as good electron traps, albeit shallow, with ionization energy of 0.025 eV for V_O/V_O^+ and 0.1 eV for V_O^+/V_O^{++}. The Fe^{2+}/Fe^{3+} energy level lies 0.8 eV below the conduction band, whereas Fe^{3+}/Fe^{4+} level exists at 2.6 eV below the conduction band [31]. Immediately after the laser illumination the shallow traps get easily ionized and the electrons get trapped at Fe^{4+} reducing it to Fe^{3+} hence increasing the Fe^{3+} concentration. With the emptying of the traps i.e, with the increase of empty oxygen vacancies, the lower valence state of Fe will be more stable enhancing the probability of $Fe^{3+} + e^- \to Fe^{2+}$ process. Therefore, the initial spike reflects the kinetics of emptying the shallow traps viz., electrons at oxygen vacancies and their trapping at Fe^{4+} sites; and the subsequent (and main) reduction of Fe^{3+} signal reflects the kinetics of $Fe^{3+} + e^- \to Fe^{2+}$ process. The genuineness of this, however, can be tested by following the decay of grating under two-beam coupling experiments.

The sudden surge of Fe^{3+}, soon after switching on the light has certain interesting consequences on the grating formation. In a two beam coupling experiment, when one of the beams is shut off the interference pattern disappears, bringing in uniform illumination. The regions which formed the 'dark' part of the interference pattern, should therefore experi-

ence the 'surge' in the concentration of Fe^{3+} which essentially should make the contrast in the phase grating more prominent despite switching off the writing beam. This was tested with E1 crystal. Figure 10 shows a typical result of a beam coupling experiment with **k** (grating vector) parallel to the c-axis. The two writing beams are designated as A_1 and A_2. When the beam A_2 was off, sudden jump in the intensity of transmitted part of A_1 (A_1t) was observed as there is no cause for energy transfer in the absence of A_2. Subsequently the transmitted part of A_1 i.e. A_1t has shown a clear reduction in intensity due to diffraction characteristic of grating formation, for the first few seconds, before the grating started to decay. These experiments were conducted with different intensity ratios of A_1 and A_2. The effect of transient grating formation is most prominent for $I_1 = I_2$ or ($m = I_1/I_2$). When the intensities are equal the contrast between dark and bright regions is highest and approaches the limit of near uniform illumination as $m \to 0$. This result is quite consistent with the EPR observation. The shorter time scale of the growth of transient grating compared to larger times scale in EPR decay was due to the effect of large differences in **k** vector in these experiments. Horowitzs *et al* [32] have reported a similar growth of a grating after the input signal was turned off in a two wave mixing experiment. They attributed it due to the formation of new grating in regions of the crystal where they could not grow earlier due to the relative weakness of the pump beam. In our model, the 'new grating' is essentially the same 'old grating' with greater contrast and thereby larger diffraction efficiency. It continued to have the same **k** vector and hence the position of the diffraction signal does not change.

6. Conclusions

We have obtained direct EPR evidence for photo-induced charge transfer from Fe^{3+} in $BaTiO_3$ at room temperature and also the involvement of defect at domain walls as sources/traps for charge carriers. The investigation of the growth and decay of Fe^{3+} has lead to the determination of the dielectric relaxation time τ_d, and also for a possible explanation for the formation of the transient grating after one of the beams is switched off in a two beam coupling experiment.

Acknowledgements

This work is assisted by the NSF, Grant # 8802971. Thanks are due to N S Dalal, Department of Chemistry, University of West Virginia, and to L D Kitspert and A S Jeevarajan of the University of Alabama at Tuscalosa for their help in providing EPR facilities in the early stage of this work.

References

[1] E Kratzig and O F Scirmer, *Chapter V – Photorefractive materials and their applications* edited by P Gunter and J P Huignard (Springer-Verlag, 1988)

[2] N V Kukhtarev, *Sov. Tech. Lett.* 2, 438 (1976)

[3] N V Kukhtarev, V B Markov, S G Odulov, M Sosskin and V L Vinetskii, *Ferroelectrics* 22, 949 (1979)

[4] G C Valley, *IEEEJ Quant. Elect.* **QE-19**, 1637 (1983)
[5] J Feinberg, D Heinman, A R Tanguay Jr and R W Hellwarth, *J. Appl.* **51**, 1297 (1980)
[6] M B Klein and G C Valley, *J. Appl. Phys.* **57**, 4901 (1985)
[7] F P Strohkendl, J M C Jonathan and R W Hellwarth, *Opt. Lett.* **11**, 312 (1986)
[8] P G Schuneman, D A Temple, R S Hatchcock, H L Tuller, H P Jenssen, D R Gable and C Warde, *J. Opt. Soc. Am.* **B5**, 1685 (1988)
[9] M H Garrett, J Y Chang, H P Jenssen and C Warde, *J. Opt. Soc. Am.* **B9**, 1407 (1992)
[10] A Abragam and B Bleany, *Paramagnetic resonance of transition ions* (Clarendon Press, 1970)
[11] E Possenriede, O F Schirmer, H J Donnerberg, G Godefroy and A Maillard, *Ferroelectrics* **92**, 245 (1989)
[12] E Posseriede, P Jacobs and O F Schirmer, *J. Phys. Condens. Matter* **4**, 4719 (1992)
[13] E Possenriede, P Jacobs, H Kröse and O F Schirmer, *Appl. Phys.* **A55**, 73 (1992)
[14] M B Klein and R N Schwartz, *J. Opt. Soc. Am.* **B3**, 293 (1986)
[15] R N Schwartz, B A Wechsler and D Rytz, *J. Am. Ceram. Soc.* **73**, 3200 (1990)
[16] B A Wechsler, D Rytz, M B Klein and R N Schwartz, *Proceedings of American Chemical Soc. (ACS)* Series No. 455, Materials for Nonlinear Optics: Chemical Perspectives, Chapter 26, ACAS (1991)
[17] R N Schwartz, B A Wechsler and R A McFarlane *Phys. Rev.* **B46**, 3263 (1992)
[18] R N Schwartz, M Ziari and S Trivedi, *Phys. Rev.* **B49**, 5274 (1994)
[19] A W Horning, R C Remple and H E Weaver, *J. Phys. Chem. Solids* **10**, 1 (1959)
[20] M D Sastry, M Moghbel and P Venkateswarlu, *Pramana – J. Phys.* **47**, 331 (1996)
[21] P Venkateswarlu, M Moghbel, M D Sastry and M Curley, Wright Laboratory WI-TR-94-500 (1994)
[22] T Sakudo, *J. Phys. Soc. Jpn.* **18**, 2109 (1964)
[23] T Sakudo and H Unoki, *J. Phys. Chem. Solids* **19**, 2109 (1964)
[24] K A Muller and W Berlinger, *Phys. Rev.* **34**, 6130 (1986)
[25] K A Muller, *Helvitica Physica Acta* **59**, 874 (1986)
[26] E S Kirkpatric, K A Muller and R S Rubins, *Phys. Rev.* **A86**, 135 (1964)
[27] Th Von Waldkirk, K A Muller and W Berlinger, *Phys. Rev.* **B5**, 4324 (1972)
[28] B A Wechsler and M B Klein, *J. Opt. Soc. Am.* **B5**, 1711 (1980)
[29] R A Mullen, *Photorefractive materials and their applications* edited by P Gunter and J P Huignard (Springer-Verlag, 1988) p. 178
[30] S Ducharme and J Feinberg, *J. Appl. Phys.* **56**, 839 (1984)
[31] M B Klien, in *Photorefractive materials and their applications* edited by P Gunter and J-P Huignard (Springer-Verlag, Berlin, Heidelberg, 1988) ch. 7
[32] M Horowitz, D Kligler and B Fisher, *J. Opt. Soc. Am.* **B8**, 2204 (1991)